Accepted Manuscript

Novel reversible methionine aminopeptidase-2 (MetAP-2) inhibitors based on purine and related bicyclic templates

Timo Heinrich, Hans-Peter Buchstaller, Bertram Cezanne, Felix Rohdich, Jörg Bomke, Manja Friese-Hamim, Mireille Krier, Thorsten Knöchel, Djordje Musil, Birgitta Leuthner, Frank Zenke

PII: S0960-894X(16)31286-0
DOI: http://dx.doi.org/10.1016/j.bmcl.2016.12.019
Reference: BMCL 24508

To appear in: *Bioorganic & Medicinal Chemistry Letters*

Received Date: 29 September 2016
Revised Date: 6 December 2016
Accepted Date: 7 December 2016

Please cite this article as: Heinrich, T., Buchstaller, H-P., Cezanne, B., Rohdich, F., Bomke, J., Friese-Hamim, M., Krier, M., Knöchel, T., Musil, D., Leuthner, B., Zenke, F., Novel reversible methionine aminopeptidase-2 (MetAP-2) inhibitors based on purine and related bicyclic templates, *Bioorganic & Medicinal Chemistry Letters* (2016), doi: http://dx.doi.org/10.1016/j.bmcl.2016.12.019

This is a PDF file of an unedited manuscript that has been accepted for publication. As a service to our customers we are providing this early version of the manuscript. The manuscript will undergo copyediting, typesetting, and review of the resulting proof before it is published in its final form. Please note that during the production process errors may be discovered which could affect the content, and all legal disclaimers that apply to the journal pertain.

ACCEPTED MANUSCRIPT

Novel reversible methionine aminopeptidase-2 (MetAP-2) inhibitors based on purine and related bicyclic templates

Timo Heinrich[a,*], Hans-Peter Buchstaller[a], Bertram Cezanne[b], Felix Rohdich[c], Jörg Bomke[a], Manja Friese-Hamim[d], Mireille Krier[a], Thorsten Knöchel[e], Djordje Musil[a], Birgitta Leuthner[a], Frank Zenke[f]

[a]Discovery Technologies, [b]Process Technologies, [c]Drug Disposition, [d]*in vivo* Pharmacology, [e]Project Management, [f]Cellular Pharmacology

Merck KGaA, Frankfurter Str. 250, D-64293 Darmstadt, Germany.

*Corresponding author Tel.: +49-6151-726589, fax: +49-6151-723129, E-mail: timo.heinrich@merckgroup.com

ACCEPTED MANUSCRIPT

ACCEPTED MANUSCRIPT

In 1990 Judah Folkman´s laboratory published a seminal discovery on the anti-angiogenic activity of the natural compound fumagillin **1**, which was isolated in 1951 from the fungus *Aspergillus fumigatus*.[1] Subsequently, intensive activities were started to improve the pharmacological and pharmaceutical properties of this compound leading to the development of a highly potent derivative TNP-470 **2** which entered clinical development in 1992 as one of the first anti-angiogenic drugs in oncology.[2,3] Although the clinical development stopped in 2001 this approach has received quite some attention ever since.[4]

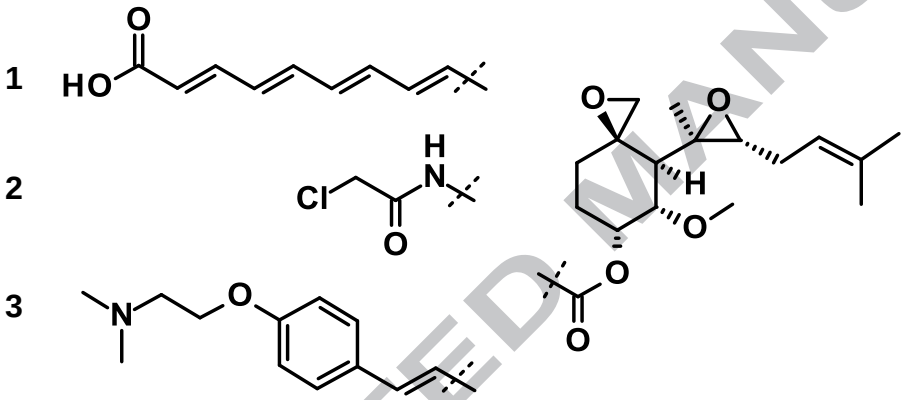

Figure 1. Irreversible MetAP-2 inhibitors: **1** (natural product fumagillin), **2** (TNP-470, former clinical development compound), **3** (beloranib, until recently under clinical investigation as anti-obesity drug).

The molecular target of fumagillin and derivatives was identified in 1997 as methionine aminopeptidase 2 (MetAP-2) by the laboratory of Craig Crews.[5] Methionine aminopeptidases are enzymes which remove the N-terminal amino acid methionine from proteins during or after the translation process. Methionine is cleaved from some but not

ACCEPTED MANUSCRIPT

all cellular proteins, especially proteins that bear a small amino acid at the second position. As part of protein maturation, cleavage is assumed to be relevant for protein stability (N-end rule) and proper function (protein folding, N-terminal myristoylation). Although, the functional relevance of N-terminal processing may be different for each affected protein and remains to be fully clarified. Three MetAPs exist in humans, MetAP-1, MetAP-2, and MAP1D. MetAP-2 is widely expressed in all human tissues, although differences exist in expression levels based on mRNA expression data. Complete knockout of MetAP-2 in mice is embryonic lethal with a pronounced block at the gastrulation stage. A tissue-restricted knockout in the endothelial cell compartment was embryonic lethal as well and showed a pronounced abnormality in vascular development,[6] indicating that MetAP-2 is important during development and required for the formation of the vascular system. Interestingly, the MetAP-2 knockout in the yeast *S. cerevisiae* is viable, but is lethal in combination with a MetAP-1 knockout, suggesting some redundancy between MetAP-1 and MetAP-2.[7] Pharmacological inhibition of MetAP-2 using different classes of inhibitors blocked proliferation of vascular endothelial cells, explaining, at least in part, the anti-angiogenic mechanism of action.[8-10]

Beside the mentioned irreversible MetAP-2 inhibitors diverse compounds were described in the literature, which inhibit MetAP-2 reversibly (Figure 2).

ACCEPTED MANUSCRIPT

ACCEPTED MANUSCRIPT

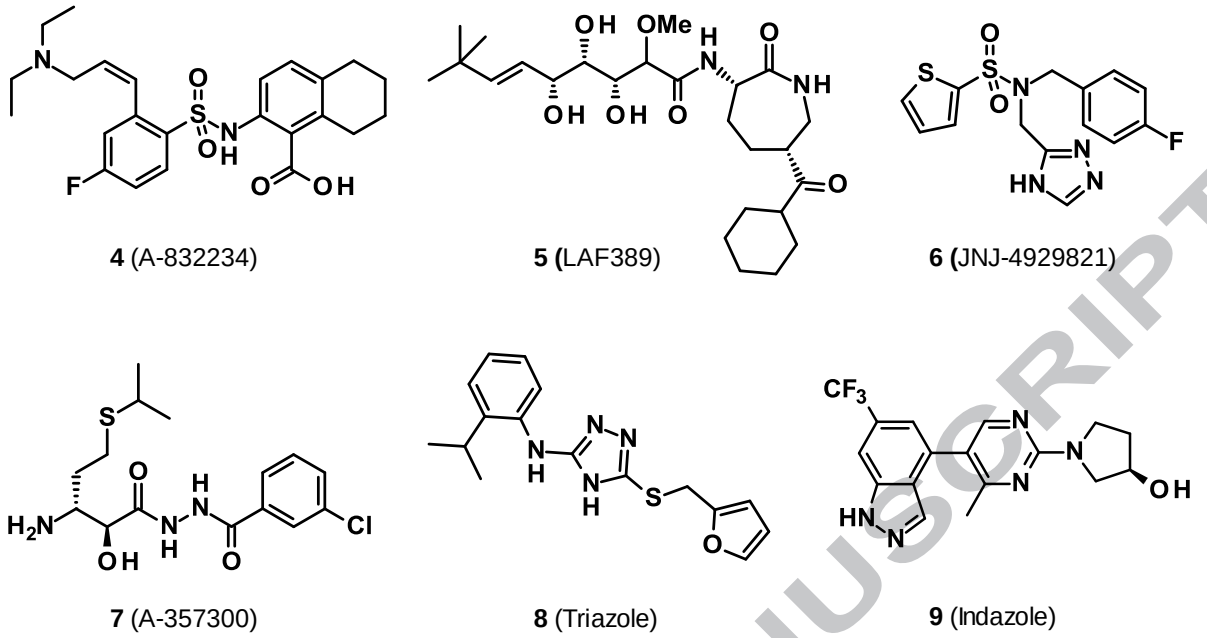

Figure 2. Reversible MetAP-2 inhibitors from different structural classes: **4** (A-832234, Anthranilic acid-sulfonamide),[11] **5** (LAF389, Bengamide),[12] **6** (JNJ-4929821, Triazole-sulfonamide),[13] **7** (A-357300, Bestatin),[17] **8** (Triazole),[14] **9** (indazole).[15]

The activity of more derivatives from each series together with their respective binding modes has been discussed in recent reviews.[16,17] Subsequently, anti-proliferative activity on some tumor cell lines has been demonstrated for MetAP-2 inhibitors indicating potential for direct anti-tumor effects as well.[8,18] The anti-proliferative effect of MetAP-2 depletion using antisense or siRNA could be confirmed by some laboratories[6,9,19] but not by others.[20] The molecular mechanism for anti-proliferative activity in endothelial and selected tumor cells is not well understood. Several intracellular events have been noted upon treatment with MetAP-2 inhibitors, such as induction of the tumor suppressor p53 and cell cycle inhibitor p21, modulation of phosphorylation of the translation initiation factor eIF-2, reduced phosphorylation of the mitogen-activated protein kinase ERK, or inhibition of non-canonical WNT signaling.[21-25] However, a consistent causality between

ACCEPTED MANUSCRIPT

target inhibition and the anti-proliferative activity could not be demonstrated so far. A wealth of published data demonstrated that MetAP-2 inhibitors have potent anti-tumor efficacy in vivo, predominantly shown in mouse models. Whether the anti-tumor efficacy in these models was indeed mediated by anti-angiogenic and/or anti-proliferative effects is not fully understood.[8,15,17,26,27] The mechanism of action, i.e. the inhibition of N-terminal protein processing, is a unique cellular response not seen with other targeted inhibitors and that's why we considered MetAP-2 as an interesting and promising tool to interfere in tumor biology and stop tumor cell proliferation.

Accordingly, the corporate compound collection was screened against the target and the 2-Cl-phenyl-ether **10** was identified as a low micromolar hit (table 1). Subsequent efforts were focused on improving potency via substitution of the phenyl ring. The synthesis of the 2-(aryloxymethyl) pyrrolidine analogues is outlined in Scheme 1 and began with the conversion of either *R*- or *S*-proline into the respective methyl esters.

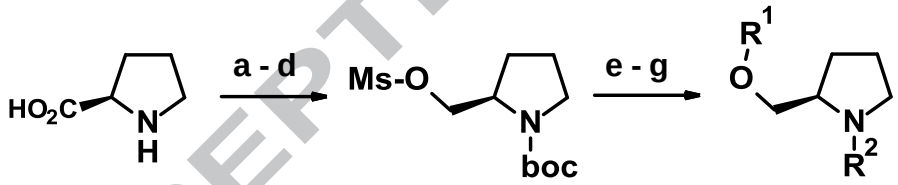

Scheme 1. Synthesis of pyrrolidine derivatives. Reagents and conditions (a) $SOCl_2$, MeOH, DMF; 0 – RT; 2h; (b) BOC_2O, TEA, *t*BuOH; 25°C, 21h; (c) LiCl, $NaBH_4$, EtOH, THF; -20°C – RT, 19 h; (d) $MeSO_2Cl$, TEA, DCM; (e) R^1-OH, Cs_2CO_3, DMF; 60°C, 16h; (f) TFA, DCM; RT, 1h; (g) R^2-Cl, for conditions see tables 1 and 2.

Protection of the nitrogen with a tert-butoxycarbonyl (Boc) group followed by reduction of the ester yielded the N-Boc-protected amino alcohols. The alcohol was converted into

ACCEPTED MANUSCRIPT

the corresponding mesylate, which was then substituted by the required phenol derivative (R^1) in the presence of cesium carbonate. After removal of the Boc group the resulting secondary amines were coupled with different commercially available bicyclic aryl-chlorides (R^2) under alternative conditions as referenced in the tables 1 and 2. Especially for the bicyclic aryl chlorides without NH-function (**22** – **25**) an alternative approach worked well: Commercially available prolinol is directly coupled to the respective bicyclic aryl chloride (conditions indicated in table 2) followed by mesylate formation of the alcohol and substitution of the latter with appropriate phenolic building blocks (R^1).

Table 1

In vitro evaluation of synthetic compounds **10** – **18**[28]

Compound	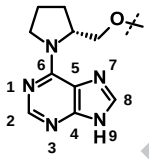	IC_{50}* [µM]
10 [a)]	2-Cl-Phe (*R*)	1 ± 0.1
11 [b)]	2-Cl-Phe (*S*)	> 50
12 [c)]	2,3-di-F-Phe	1.6 ± 0.1
13 [c)]	3-F-Phe	2 ± 0.1
14 [d)]	4-F-Phe	3.8 ± 2.5
15 [c)]	4-CN-Phe	1.3 ± 0.3

ACCEPTED MANUSCRIPT

16 [b)]	2-Me-Phe	0.7 ± 0.2
17 [a)]	1-naphthyl	0.45 ± 0.1
18 [a)]	5-isoquinolinyl	0.23 ± 0.1

* Activity in recombinant MetAP-2 enzyme assay. Mean of three determinations. Coupling conditions of the pyrrolidine to the bicyclic aryl-chloride (R^2-Cl): a) DIPEA, 1-butanol, 6.5 h, 120 °C, MW; b) TEA, 1-butanol, 1 h, 100 °C; c) acetone, 20 min, 150 °C, MW; d) diglyme, 20 min, 150 °C, MW;

The *S*-enantiomer **11** of the screening hit is inactive and hence further optimization work focused on *R*-isomers. The biochemical activity of the halogen bearing hit-analogs **12**, **13** or **14** is in the same range as initial hit **10**, which suggests that changes in substituent size and different inductive electron withdrawing residues on the aryl moiety have no impact on ligand binding. Increasing electron density in the phenyl ring with a small aliphatic moiety like in **16** provided an improvement in activity, while further extension of the residue to the naphthalene system (**17**) resulted in even greater enzyme potency. However, when considering lipophilic ligand efficiency (LLE),[29] it is obvious that the larger molecule **17** only shows minimal improvement (LLEs: **16** = 2.11; **17** = 2.06). Nevertheless, the naphthalene moiety was used as the basis for further optimization of enzyme potency, initially via increasing molecular polarity by introduction of a nitrogen into the bicyclic ring. An isoquinoline derivative (**18**) validated these efforts with an improved enzyme activity, which is also reflected in an improvement of the LLE (2.71).

ACCEPTED MANUSCRIPT

Explorations of the ether-linker between the pyrrolidine bridge and the extended aryl moiety itself did not improve activity. Alkane, alkene, amine, amide and ester were tested, but turned out to be less potent.[30]

In a parallel approach the initial hit **10** was used as template to investigate the structural activity relationship of the purine core. Even subtle substitutions like introduction of a methyl group in positions 2 or 8 led to completely inactive compounds. Same is true for the introduction of fluorine or amine in position 2.[30] Structural analysis (vide infra) had shown, that the purine nitrogens N3 and N9 are in contact to the metal ions in the active site of the enzyme. Accordingly, it was anticipated that manipulations of the π-electron distribution of the bicyclic template should influence metal ion interaction and hence activity (table 2).

Table 2.

In vitro evaluation of synthetic compounds **19** – **27** [28]

Compound	Structure	IC_{50}* [µM]
19 a)	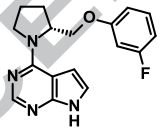	> 50
20 b)	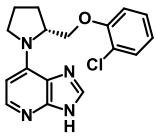	2.2 ± 0.7

ACCEPTED MANUSCRIPT

21 [c]	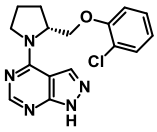	8.6 ± 2.1
22 [d]	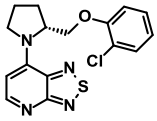	2.8 ± 0.6
23 [e]	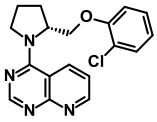	> 50
24 [e]	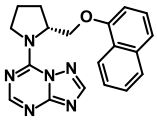	1.8 ± 0.2
25 [f]	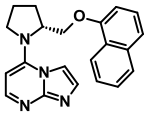	0.56 ± 0.1
26 [f]	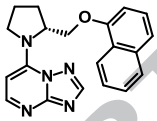	0.11 ± 0.01
27 [g]	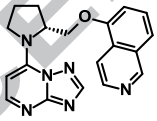	0.038 ± 0.001

* Activity in recombinant MetAP-2 enzyme assay. Mean of three determinations. Coupling conditions of the pyrrolidine to the bicyclic aryl-chloride (R^2-Cl): a) Acetone, 20 min, 150 °C, MW; b) TEA, 1-butanol, 40 min, 150 °C, MW; c) TEA, 1-butanol, 1.5 h, 100 °C; d) neat 100 °C, 12 h;[31] e) Cs_2CO_3, ACN, 6 h, RT; e) generation from

ACCEPTED MANUSCRIPT

alcohol with benzyltributylammoniumbromide, isopropyl acetate, ACN and $POCl_3$, 1.5 h, 65 °C; f) TEA, 1-butanol, 100 min, 120 °C, MW; g) Cs_2CO_3, DMF, 80 °C, 12 h.

For the 7H-pyrrolo[2,3-d]pyrimidine derivative **19**, the N9 atom of the purine system is replaced by a carbon atom, fixing thereby the proton to the remaining nitrogen in the five membered ring. As this is incompatible with coordination to the active site cation, the compound is inactive as expected. Compound **20** is a 3H-imidazo[4,5-b]pyridine where N1 of the original purine was replaced by a carbon atom. This modification has no significant effect on binding affinity as both compounds **10** and **20** are equally active. Moving purine nitrogen N7 into position 8 to get the 1H-pyrazolo[3,4-d]pyrimidine core in **21** reduces affinity to 8.6 µM. Probably only the 2H-tautomer can efficiently bind to the active site, and this tautomer state might be energetically unfavorable per se. Compound **22** represents a [1,2,5]thiadiazolo[3,4-b]pyridine bearing a sulfur in the five membered ring between the nitrogens. This compound is equipotent as its carbon analog **20**. Widening the angle of the five membered ring and increasing π-electron density by the sulfur atom has no positive impact on MetAP-2 binding. In addition, this is the first scaffold replacement where not other tautomeric form is expected as no hydrogen atom to a heteroatom needs to be allocated appropriately. Also, the pyrido[2,3-d]pyrimidine derivative **23** bears no heteroatom-hydrogen and only lone pair donors. However, for this molecule, the second six membered ring is not tolerated and the compound is inactive. The introduction of a nitrogen atom in the bridge head position 5 of the bicyclic system with a 6 and 5 membered ring allows the removal of the nitrogen bound hydrogen without introducing an additional heteroatom. At this point, introduction of the

ACCEPTED MANUSCRIPT

active naphthalene moiety (from compound **17**) was evaluated in subsequent purine core modifications to further drive enzymatic potency. Interestingly, it was observed that the [1,2,4]triazolo[1,5-a][1,3,5]triazine analog **24** is 3 fold less active than compound **17**. It can be speculated that the high nitrogen loading of the aryl template induced a reduced electron density on nitrogens 3 and 9 that could be responsible for the activity. This consideration was confirmed when replacing the two nitrogens in positions 1 and 7 providing the imidazo[1,2-a]pyrimidine **25**, a moleculde with sub-µM enzymatic activity. Subsequent systematic exploration of the bicyclic core moiety and introduction of a nitrogen in the five membered ring gave the [1,2,4]triazolo[1,5-a]pyrimidine **26** with improved activity. Finally, increasing polarity in the naphthalene moiety by substitution with the isoquinoline known from **18** resulted in compound **27** which possessed two digit nM MetAP-2 activity.[32] This improvement is confirmed with the LLE of 4.2 for **27**. Extended profiling of the most potent derivatives revealed that *in vitro* properties are in an acceptable range. The thermodynamic solubility of the optimized hit **27** is 171 µg/ml and its permeability in the Caco-2 assay is 21E-6 cm/s with an efflux ratio of 2.9.

The crystallization of derivatives from this series with the MetAP-2 protein helped to rationalize the impact of the extended aryl moiety on affinity. As shown in figure 3 (PDB: 5LYW), the 2-methyl-phenyl ether of **16** is in π-stacking interaction with His339 and Tyr444. Obviously, the contribution of this π-electron interaction to affinity is more favorable for electron rich aryl-ethers of the ligand like in **16** and **17** than for electron poor aromatic systems (**13**, **15**).

ACCEPTED MANUSCRIPT

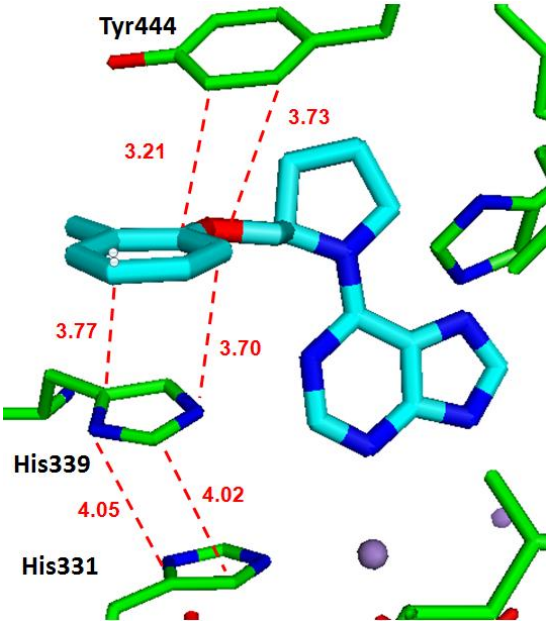

Figure 3.[33] XRay structure analysis of **16** bound to human MetAP-2. The distances between the amino acid side chains and the aryl residue of the ether are given in Ångstrom. The Mn^{2+} ions are depicted in purple. The distance from N3 to the closest ion is 2.35 Å and from N9 2.39 Å. The distance between the metal cores is 3.24 Å.

Interestingly, the imidazole of His339 is sandwiched in a co-planar manner between the aryl moiety of ligand **16** and imidazole of His331 (figure 4 A). Capturing the His339 side chain in this conformation is unprecedented.[34] For the published MetAP-2 structures e.g. the apo form (PDB: 1BN5), a T-shaped orientation of the His339-imidazole edge to the face of His331-imidazole is found (figure 4 B).

ACCEPTED MANUSCRIPT

ACCEPTED MANUSCRIPT

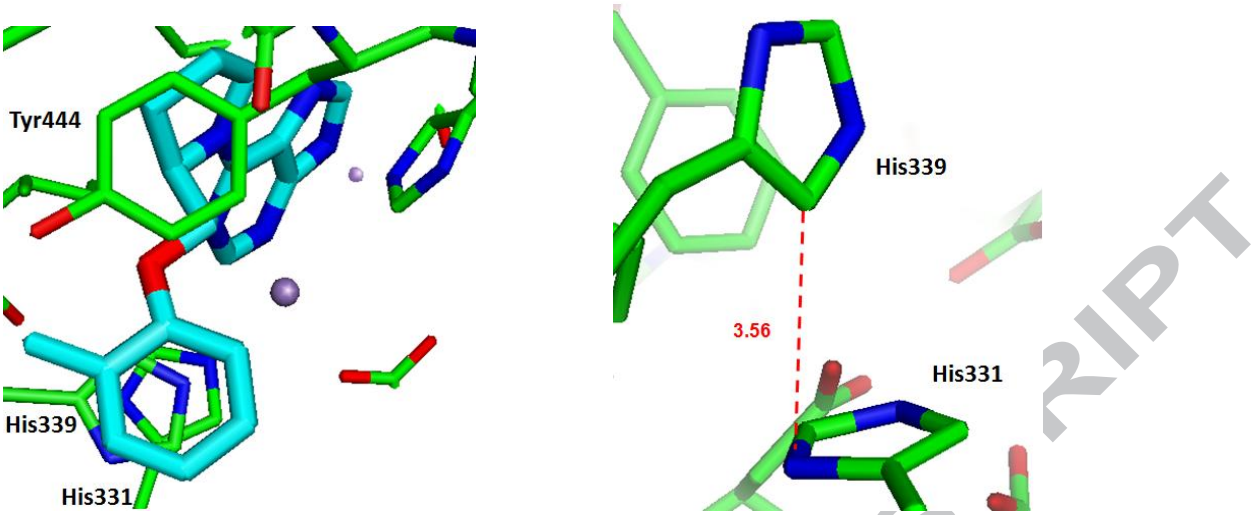

A B

Figure 4.[33] **A**. Depiction of imidazole from His339 sandwiched between the imidazole of His331 and the 2-tolyl residue of **16**. **B**. Apo-structure of human MetAP-2 shows T-shaped orientation between the two imidazoles of His339 and His331.

For other ligands with structural data in the PDB, the imidazole of His339 is pushed out of the active site as shown in figure 5 for the irreversible MetAP-2 inhibitor **2** (TNP-470, figure 5 A; PDB: 1B6A) or the anthranilic acid derivative **4** (A-849519, figure 5 B; PDB: 1YW9).[11]

ACCEPTED MANUSCRIPT

ACCEPTED MANUSCRIPT

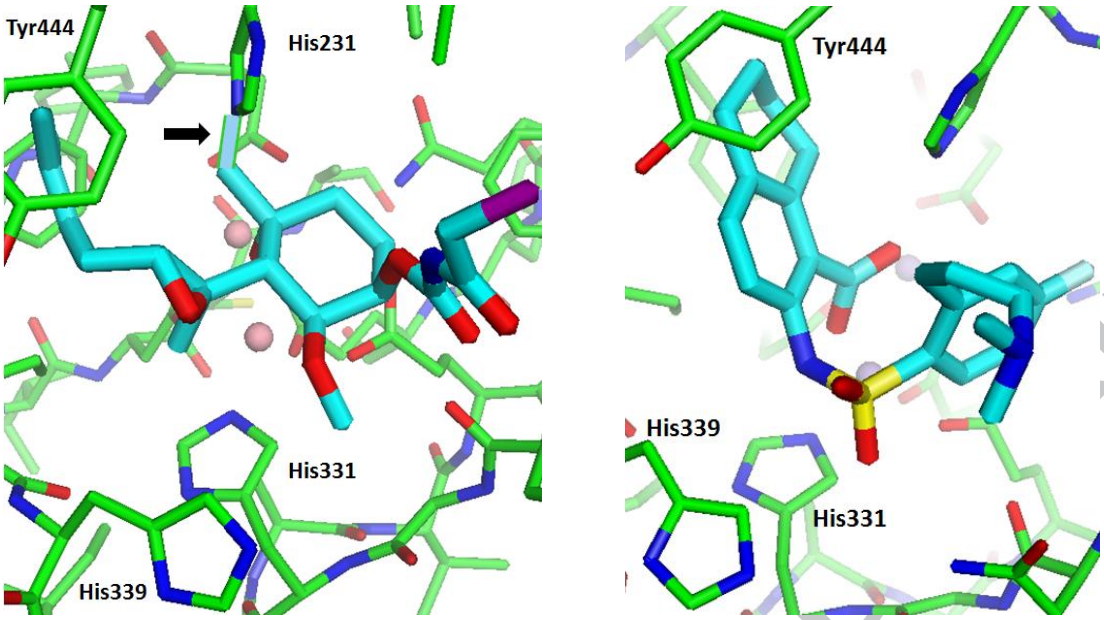

A **B**

Figure 5.[33] Xray structure analyses of human MetAP-2 with **A**. TNP-470 (shortest distance between imidazoles of His339 and His331 is 4.52 Ångstrom – not shown here; the covalent bond between the imidazole of His231 and the ligand is indicated with the black arrow) **B**. A849519 (shortest distance between imidazoles is 4.55 Ångstrom – not depicted explicitly)

Beside the analysis of interactions at the entrance to the active site, we investigated the impact of core modifications on activity and therefore analyzed the structure of **16** bound to MetAP-2. The result is shown in figure 6. From figure 6A one could assume that there is some space in the back of the binding pocket. Small substituents on the purine core in position 2 or 8 (indicated by the yellow arrow in figure 6) like fluorine or methyl give only inactive compounds suggesting that the embodiment of the pocket does not leave room for any substitution or does disrupt a water cluster in an unfavorable manner.

ACCEPTED MANUSCRIPT

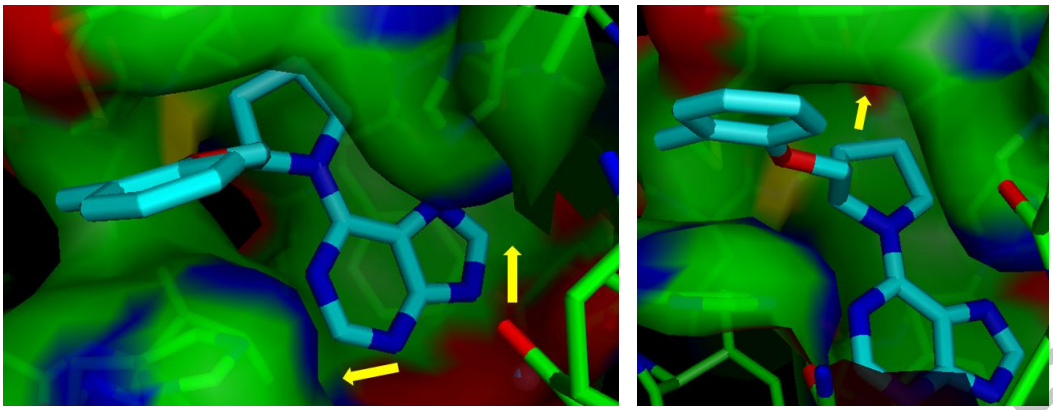

A B

Figure 6.[33] **16** bound to MetAP-2 with protein surface is shown. The yellow arrows indicate where additional space around the purine template (A) or the pyrrolidine (B) is anticipated

Also, the methionine binding pocket of the enzyme where the pyrrolidine of the inhibitor is positioned suggests additional space (figure 6B). Neither mono- nor di-fluoro substitution or hydroxy- or keto-functionality in position 4 of the saturated ring improved activity.[30] The pyrrolidine moiety itself was examined in more detail i.e. ring size was varied from azetidines via piperidines up to azepines. In all cases, no improvement of activity could be found.[30] This was considered remarkable, especially after analysis of the binding mode of this compound class. Fluorine substitution on the pyrrolidine is filling the methionine binding pocket and should increase the contact surface with the protein resulting in higher affinity. Steric clashes were not considered to occur. The proximate binding site above the metal ions is quite rigid as well as the more distal methionine side chain binding pocket. But the latter can be addressed via an alternate vector as the

ACCEPTED MANUSCRIPT

analysis of the crystal structure of **27** proved (figure 7; PDB code for structure of **27**: 5LYX).

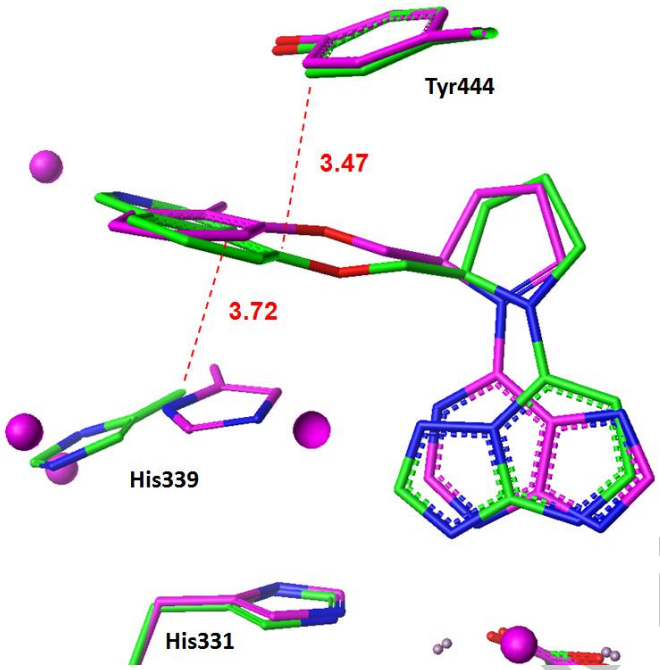

Figure 7.[33] Superposition of the purine based derivative **16** (magenta) and the [1,2,4]Triazolo[1,5-a]pyrimidine heterocycle of **27** (green). The bicyclic scaffold is flipped by 180° for the latter compared to the orientation of the purine core.

The depiction in figure 7 illustrates the 180° turn of the metal binding template when modifying the NH bearing purine (magenta in figure 7) into the triazolo[1,5-a]pyrimidine without any heteroatom bound proton (green in figure 7). This was remarkable since the initial assumption has been that a six-membered ring in the back of the pocket was not favorable since compound **23** was inactive. From the triazolo[1,5-a]pyrimidine scaffold, the pyrrolidine moiety enters the methionine pocket from a slightly more buried position compared to the situation when the pyrrolidine is bound to the purine core. Another

ACCEPTED MANUSCRIPT

notable change in orientation can be observed in figure 7: the imidazole side chain of His339 is pushed out of π-π interactions discussed in figure 3. The closest contact between the imidazole of His339 and the isoquinoline of **27** is 4.56 Å (not indicated in the figure) and the methylene-carbon of the amino acid side chain is close to C3 of the isoquinoline (3.72 Å). The linking C5 of the isoquinoline is 3.47 Å away from the closest carbon of Tyr444, whereas the toluene of **16** is in 3.21 Å distance to the phenol of Tyr444 (figure 3). Accordingly, the hydrophobic interactions of the ether moiety presented on the triazolo[1,5-a]pyrimidine (**27**) contribute to lesser extend to the binding affinity than the purine bound ether residue. This binding mode of the triazolo[1,5-a]pyrimidine scaffold had been observed also by others using our MetAP-2 inhibitors in the context of their investigations.[15]

In this study the original purine based MetAP-2 screening hit **10** was used as the basis for multiple optimization approaches. Only the R-configuration at the pyrrolidine is tolerated in the active site of MetAP-2. Pyrrolidine decorations did not improve activity. Hence the saturated five-membered ring fills the lipophilic methionine binding-pocket optimally. Moreover, variations of the $-CH_2-O-$ bridge had no beneficial effect on potency. Optimization of the aryl moiety attached to the ether contributed to an increased activity. Extension of the monocyclic ring to the bicyclic moiety proved to be most favorable to capture His339 side chain in an unprecedented fashion and improve binding by sandwiching this imidazole of His339 between the imidazole of His331 and the aryl-ether of the ligand. The purine core is suitable when the 7H tautomer is accessible. Small substituents on this template are not tolerated. An optimized nitrogen-positioning within the indene-scaffold contributes to an improved activity. The best activity was obtained with the [1,2,4]triazolo[1,5-a]pyrimidine template which was

ACCEPTED MANUSCRIPT

identified via systematic investigations. Remarkably, the orientation of the bicyclic metal binding template flipped by 180° when the original purine core was optimized into a scaffold without any nitrogen-bound proton. Hydrophobic interactions of the isoquinoline ether of **27** with Tyr444 and His339 are less pronounced compared to the VdW contacts of the tolyl ether of **16**. The outlined optimization enabled the generation of biochemical active compounds with acceptable to favorable *in vitro* properties and paved the way for further optimizations that will be discussed in due course.

ACCEPTED MANUSCRIPT

ACCEPTED MANUSCRIPT

References and notes

1. Ingber, D.; Fujita, T.; Kishimoto, S.; Sudo, K.; Kanamaru, T.; Brem, H.; Folkman, J. *Nature* **1990**, *348*, 555.
2. Kruger, E. A.; Figg, W. D. *Expert. Opin. Investig. Drugs* **2000**, *9*, 1383.
3. Bhargava, P.; Marshall, J. L.; Rizvi, N.; Dahut, W.; Yoe, J.; Figuera, M.; Phipps, K.; Ong, V. S.; Kato, A.; Hawkins, M. J. *Clin. Cancer Res.* **1999**, *5*, 1989.
4. Selvakumar , P.; Lakshmikuttyamma, A.; Dimmock, J. R.; Sharma, R. K. *Biochim. Biophys. Acta* **2006**, *1765,* 148.
5. Sin, N.; Meng, L.; Wang, M. Q. W.; Wen, J. J.; Bornmann, W. G.; Crews, C. M. *Proc. Natl. Acad. Sci. USA* **1997**, *94*, 6099.
6. Yeh, J.-R. J.; Ju, R.; Brdlik, C. M.; Zhang, W.; Zahng, Y.; Matyskiale, M. E.; Shotwell, J. D.; Crews, C. M. *Proc. Natl. Acad. Sci. USA* **2006**, *103*, 10379.
7. Li, X.; Chang, Y.-H. *Proc. Natl. Acad. Sci. USA* **1995**, *92*, 12357.
8. Wang. J.; Tucker, L. A.; Stavropoulos, J.; Zhang, Q.; Wang, Y.-C.; Bukofzer, G.; Niquette, A.; Meulbroek, J. A.; Barnes, D. M.; Shen, J.; Bouska, J.; Donawho, C.; Sheppard, G. S.; Bell, R. L. *Proc. Natl. Acad. Sci. USA* **2008**, *105*, 1838.
9. Bernier, S. G.; Taghizadeh, N.; Thompson, C. D.; Westlin, W. F.; Hannig, G. *J. Cell Biochem.* **2005**, *95*, 1191.
10. Ehlers, T.; Furness, S.; Robinson, T. P.; Zhong, H. A.; Goldsmith, D.; Aribser, J.; Bowen, J. P. *Curr. Top. Med. Chem.* **2016**, *16*, 1478.
11. Sheppard, G. S.; Wang, J.; Kawai, M.; Fidanze, S. D.; BaMaung, N. Y.; Erickson, S. A.; Barnes, D. M.; Tedrow J. S.; Kolaczkowski, L.; Vasudevan, A.; Park, D. C.; Wang, G. T.; Sanders, W. J.; Mantei, R. A.; Palazzo, F.; Tucker-Garcia, L.; Lou, P.; Zhang, Q.; Park, C. H.; Kim, K. H.; Petros, A.; Olejniczak, E.; Nettesheim, D.; Hajduk, P.; Henkin, J.; Lesniewski, R.; Davidsen, S. K.; Bell, R. L. *J. Med. Chem.* **2006**, *49*, 3832.
12. Xu, W.; Lu, J.-P.; Ye, Q.-Z. *J. Med. Chem.* **2012**, *55*, 8021.
13. Garrabrand, T.; Tuman, R. W.; Ludovici, D.; Tominovich, R.; Simoneaux, R. L.; Galemmo, R. A. Jr.; Johnson, D. L. *Angiogenesis* **2004**, *7*, 91.
14. Marino, J. P. Jr.; Fisher, P. W.; Hofmann, G. A.; Kirkpatrick, R. B.; Janson, C. A.; Johnson, R. K.; Ma, C.; Mattern, M.; Meek, T. D.; Ryan, M. D.; Schulz, C.; Smith, W. W.; Tew, D. G.; Tomazek, T. A. Jr.; Veber, D. F.; Xiong, W. C.; Yamamoto, Y.; Yamashita, K.; Yang, G.; Thompson, S. K. *J. Med. Chem.* **2007**, *50*, 3777.
15. Cheruvallath, Z.; Tang, M.; McBride, C.; Komandla, M.; Miura, J.; Ton-Nu, T.; Erikson, P.; Feng, J.; Farrell, P.; Lawson, J. D.; Vanderpool, D.; Wu, Y.; Dougan, D. R.; Plonowski, A.; Holub, C.; Larson, C. *Bioorg. Med. Chem. Lett.* **2016**, *26*, 2774.
16. Yin, S.-Q.; Wang, J.-J.; Zhang, C.-M.; Liu, Z.-P. *Curr. Med. Chem.* **2012**, *19*, 1021.
17. Mauriz, J. L.; Martin-Renedo, J.; Garcia-Palomo, A.; Tunon, M. J.; Gonzalez-Gallego, J. *Curr. Drug Targets* **2010**, *11*, 1439.
18. Wang, J.; Sheppard, G. S.; Lou, P.; Kawai, M.; BaMaung, N.; Erickson, S. A.; Tucker-Garcia, L.; Park, C.; Bouska, J.; Wang, Y.-C.; Frost, D.; Tapang, P.; Albert, D. H.; Morgan, S. J.; Morowitz, M.; Shusterman, S.; Maris, J. M.; Lesniewski, R.; Henkin, J. *Cancer Res.* **2003**, *63*, 7861.
19. Datta, B.; Datta, R. *Exp. Cell Res.* **1999**, *246*, 376.
20. Kim, S.; LaMontagne, K.; Sabio, M.; Sharma, S.; Versace, R. W.; Yusuff, N.; Phillips, P. E. *Cancer Res.* **2004**, *64,* 2984.

ACCEPTED MANUSCRIPT

21. Zhang, Y.; Griffith, E. C.; Sage, J.; Jacks, T.; Liu, J. O. *Proc. Natl. Acad. Sci. USA* **2000**, *97*, 6427.
22. Datta, B.; Majumdar, A.; Datta, R.; Balusu, R. *Biochemistry* **2004**, *43*, 14821.
23. Zhang, Y.; Yeh, J. R.; Mara, A.; Ju, R.; Hines, J. F.; Cirone, P.; Griesbach, H. L.; Schneider, I.; Slusarski, D. C.; Holley, S. A.; Crews, C. M. *Chem.Biol.* **2006**, *13,* 1001.
24. Datta, B.; Ghosh, A.; Majumdar, A.; Datta, R. *Biochemistry* **2007**, *46*, 3465.
25. Sundberg, T. B.; Darricarrere, N.; Cirone, P.; Li, X.; McDonald, L.; Mei, X.; Westlake, C. J.; Slusarski, D. C.; Beynon, R. J.; Crews, C. M. *Chem.Biol.* **2011**; *18*, 1300.
26. Chun, E.; Han, C. K.; Yoon, J. H.; Sim, T. B.; Kim, Y.-K.; Lee, K.-Y. *Int. J. Cancer* **2005**, *114*, 124.
27. Tucker, L. A.; Zhang, Q.; Sheppard, G. S.; Lou, P.; Jiang, F.; McKeegan, E.; Lesniewski, R.; Davidsen, S. K.; Bell, R. L.; Wang, J. *Oncogene* **2008**, *27*, 3967.
28. Biochemical activity testing of MetAP-2: MetAP-2 activity was determined by an enzyme coupled assay using the tripeptide Met-Ala-Ser (MAS) as substrate and recombinant human MetAP-2 (His-Tev-MetAP-2, prepared in-house). The released methionine is converted by L-amino acid oxidase (AAO) to Met ox and hydrogen peroxide is released. In a second step horse radish peroxidase catalyses the oxidation of the leuko dye dianisidine to dianisidine ox with hydrogen peroxide as co-substrate. The produced dianisidine ox was detected photometrically as increase in absorbance at 450 nm. MetAP-2 activity was determined in a kinetic measurement mode. The release of one molecule methionine corresponds to the production of one molecule dianisidine ox. The MetAP-2 enzymatic activity is directly corresponding to the increase in absorbance per time. In detail, the assay was performed in 384 well microtiter plate (Greiner 78110 MTP, transparent) in a total reaction volume of 50 µl at 22 °C. 0.35 µg of N-terminal His tag human rec MetAP-2 (prepared in house, aa 2-478, fc 123 nM), 1 u horse radish Peroxidase (Roche, Mannheim), 0.02 u L-amino acid oxidase (Sigma-Aldrich, St.Louis), 0.6 mM Dianisidine (Sigma-Aldrich, St. Louis, dissolved in 50 mM HCl, 10% DMSO) were incubated in the absence or presence of the test compound (10 dilution concentrations) in 100 mM Hepes, 50 mM NaCl, 50 µM $MnCl_2$ at pH 7.0 for 15 min at 22 °C (According to the discussion in the literature we considered manganese as the relevant metal co-factor Wang, J.; Sheppard, G. S.; Lou, P.; Kawai, M.; Park, C.; Egan, D. A.; Schneider, A.; Bouska, J.; Lesniewski, R.; Henkin, J. *Biochem*. **2003**, *42*, 5035). The reaction was started by the addition of 500µM (fc) MAS peptide (Sigma-Aldrich, St. Louis). After mixing the first measurement of absorbance was performed on an Envision multimode reader (Perkin –Elmer LAS Germany GmbH) at wavelength of 450 nm. The reaction was incubated at 22 °C for additional 45 min and the second absorbance measurement was performed. The increase of absorbance per time was determined. The control value used was the inhibitor- free reaction with 0.5 % DMSO (fc). As pharmacological inhibitor control Fumagillin (Sigma-Aldrich, St.Louis) in a final concentration of 5 µM was used. The inhibitory values (IC_{50}) were determined using the program Condosseo® from GeneData.
29. Ryckmans, T.; Edwards, M. P.; Horne, V. A.; Correia, A. M.; Owen, D. R.; Thompson, L. R.; Tran, I.; Tutt, M. F.; Young, T. *Bioorg. Med. Chem. Lett.* **2009**, *19*, 4406.
30. Because of missing enzymatic activity compounds are not discussed in more detail.
31. Sharma, K. S. *Indian J. Chem., Section B*, **1979**, 17, 13.
32. Synthesis of **27**: To 2 °C cold H_2SO_4 (270 ml) was first added racemic malic acid (80 g, 596 mmol) without temperature increase above 10 °C and in the same way 3-amino-1H-1,2,4-triazole (50 g, 595 mmol). The mixture was stirred for 12 h at RT and finally heated

ACCEPTED MANUSCRIPT

to 100 °C for 1h, giving a clear yellow solution. The cold mixture was poured on ice, pH was adjusted to 6 with conc. NaOH solution and the precipitate was filtered off, washed with cold water and dried, giving 35 g colorless crystals of [1,2,4]triazolo[1,5-a]pyrimidin-7-ol. At RT the alcohol (6.5 g, 48 mmol) was given slowly to $POCl_3$ (30 ml) and then heated to reflux for 1.5 h, giving a clear solution. All volatile parts were removed in vacuum and the remainder was poured on ice-water cautiously. The well stirred mixture was treated with conc. NaOH solution to reach pH = 8. The precipitate was filtered off and the liquid fraction were re-extracted with ethylacetate. The combined solid fractions were dried to 5 g of 7-chloro-[1,2,4]triazolo[1,5-a]pyrimidine. A solution of 1-butanol (120 ml) with 7-chloro-[1,2,4]triazolo[1,5-a]pyrimidine (6.2 g, 40 mmol) and D-prolinol (4 g, 39 mmol) was heated for 3 h to 120 °C in the microwave with increased pressure up to 10 bar. After solvent removal and silica gel chromatography 8.4 g of yellow crystals were obtained. [(2R)-1-([1,2,4]triazolo[1,5-a]pyrimidin-7-yl)pyrrolidin-2-yl]methanol (4 g, 18 mmol) was dissolved in CDM (40 ml) and TEA (5.8 ml) was added. At 0 °C a solution of methanesulfonyl chloride (2.8 ml; 36 mmol) in CDM (10 ml) was added slowly. After complete addition the mixture was stirred at RT for 12 h. After aqueous extraction the organic phase was evaporated to dryness and purified by chromatography giving the product as brown oil (2.2 g). A suspension of [(2R)-1-([1,2,4]triazolo[1,5-a]pyrimidin-7-yl)pyrrolidin-2-yl]methyl methanesulfonate (250 mg, 0.8 mmol), isoquinolin-5-ol (120 mg, 0.8 mmol) and cesium carbonate (1 g, 3 mmol) in DMF (20 ml) was heated to 80 °C for 12 h. After solvent removal and aqueous work up the organic phase was evaporated and purified by chromatography to give 5-[[(2R)-1-([1,2,4]triazolo[1,5-a]pyrimidin-7-yl)pyrrolidin-2-yl]methoxy]isoquinoline **27** as beige solid (120 mg). ^{1}H NMR (500 MHz, DMSO-d_6) δ 9.24 (s, 1H), 8.47 – 8.39 (m, 2H), 8.31 (d, J = 5.7 Hz, 1H), 7.64 (d, J = 8.2 Hz, 1H), 7.54 (m, 2H), 7.23 (d, J = 7.7 Hz, 1H), 6.43 (d, J = 5.7 Hz, 1H), 5.72 (s, 1H), 4.44 (dd, J = 9.8, 5.0 Hz, 1H), 4.25 (dd, J = 9.8, 6.4 Hz, 1H), 4.00 (br. s, 1H), 3.80 (br. s, 1H), 2.27 (m, 3H), 2.11 (m, 1H). Mp.: 158 – 159 °C.

33. PDB visualization tool: Benchware® 3D Explorer 2.7; JPR Technologies
34. Unconstrained flex docking with CCDC Gold Suite v. 5.4.1 did not predict the observed XRay pose.

ACCEPTED MANUSCRIPT

ACCEPTED MANUSCRIPT

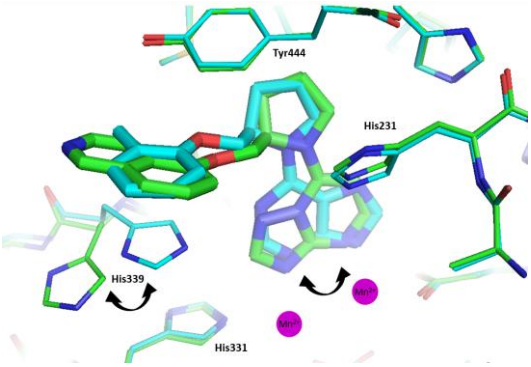

Both, the purine and the triazolopyrimidine based MetAP-2 inhibitors coordinate the manganese ions in the active site but the 5/6 membered bicyclic ring system is flipped by 180°C. When binding the latter the imidazole side chain of His339 is pushed out of its conformation with the purine MetAP-2 inhibitor.

ACCEPTED MANUSCRIPT